

Time-Domain Geometric Eddy-Current A Formulation for Hexahedral Grids

Lorenzo Codecasa¹, Patrick Dular², Ruben Specogna³, and Francesco Trevisan³

¹Dipartimento di Elettronica ed Informazione, Politecnico di Milano, Milano 20133, Italy

²Department of Electrical Engineering and Computer Science, Université de Liège, Liège 4000, Belgium

³Dipartimento di Ingegneria Elettrica, Gestionale e Meccanica (DIEGM), Università di Udine, Udine 33100, Italy

The aim of this paper is to present a 3-D time-domain eddy-current A formulation based on the discrete geometric approach (DGA) over unstructured and nonorthogonal hexahedral dual grids. The resulting differential algebraic system of equation, solved by means of a singly-diagonally implicit Runge–Kutta (SDIRK) variable step-size solver, leads to very accurate results at reduced computational costs, as shown by numerical analysis.

Index Terms—Cell method (CM), discrete geometric approach (DGA), eddy currents, finite integration technique (FIT), time domain.

I. INTRODUCTION

THE so-called discrete geometric approach (DGA) [1], common to the finite integration technique (FIT) [2], [3] or the cell method (CM) [4], [5], allows to solve directly Maxwell's equations in an alternative way with respect to the classical Galerkin method in finite elements.

In [6], Codecasa *et al.* have proposed a novel method for discretizing the constitutive relations of the DGA for generic hexahedral dual grids. As a major theoretical result, such method guarantees the consistency and the stability of the discretized equations, in the sense of Lax–Richtmyer equivalence theorem [7].

In this paper, such novel method for discretizing constitutive relations is applied to eddy-current problems in the time domain. In this way, an A formulation for eddy-current problems in the time domain is derived by the DGA, for unstructured and nonorthogonal dual grids, in which the primal grid is hexahedral. As far as the authors know, this is a major achievement with respect to previous results reported in literature [8], [9], in which eddy-current problems were discretized by DGA only over *structured hexahedral grids*. As shown by the proposed numerical analysis, the novel constitutive relations can lead to very accurate results at reduced computational costs, since they avoid the geometric discretization inaccuracy deriving from the use of orthogonal hexahedral grids [8], such as staircase effects, or from the use of *structured hexahedral grids* for modeling complex geometries [9].

II. DGA FORMULATION

The 3-D domain of interest D of the eddy-current problem is covered by a mesh of generic hexahedra. The corresponding cell complex [4] is denoted as \mathcal{K} . Three subdomains of D are identified: the passive conductive region D_c , the nonconductive

region (air region) D_a , and the source region D_s . From \mathcal{K} , a dual complex $\tilde{\mathcal{K}}$ is also introduced [4], based on the barycentric subdivision of the boundary of each hexahedron [10]. The incidence matrix between faces and edges is denoted by \mathbf{C} and the incidence matrix between hexahedra and faces is denoted by \mathbf{D} . The incidence matrix between faces and edges of the dual complex is $\tilde{\mathbf{C}} = \mathbf{C}^T$ [4].

Next, the following integrals of the field quantities with respect to the oriented geometric elements of the mesh are introduced, yielding the degrees of freedom (DoF) arrays:

- Φ is the array of magnetic fluxes associated with faces $f \in D$;
- \mathbf{F} is the array of magnetomotive forces (m.m.f.s) associated with dual edges $\tilde{e} \in D$;
- \mathbf{A} is the array of circulations of the magnetic vector potential A along primal edges $e \in D$;
- \mathbf{I} is the array of currents associated with dual faces \tilde{f} in D_c ;
- array \mathbf{I}_s of impressed currents associated with dual faces \tilde{f} is introduced in D_s ;
- finally \mathbf{U} is the array of electromotive forces (e.m.f.s) on primal edges $e \in D_c$.

Maxwell's laws are written *exactly* as topological balance equations between DoFs arrays, as

$$\begin{aligned} (\tilde{\mathbf{C}}\mathbf{F})_e &= 0, & e \in D_a \\ (\tilde{\mathbf{C}}\mathbf{F})_e &= (\mathbf{I}_s)_e, & e \in D_s \end{aligned} \quad (1)$$

$$\begin{aligned} (\tilde{\mathbf{C}}\mathbf{F})_e &= (\mathbf{I})_e, & e \in D_c \\ (\Phi)_f &= (\mathbf{C}\mathbf{A})_f, & f \in D \end{aligned} \quad (2)$$

where (1) is the Ampère law, and (2) involves the array \mathbf{A} in such a way that Gauss' law $\mathbf{D}\Phi = 0$ is satisfied identically (since $\mathbf{D}\mathbf{C} = 0$). Discrete Faraday's law

$$(\mathbf{C}\mathbf{U})_f = -\frac{d}{dt}(\Phi)_f, \quad e \in D_c \quad (3)$$

is formulated, in terms of \mathbf{A} , as follows:

$$(\mathbf{U})_e = \left(-\frac{d\mathbf{A}}{dt} \right)_e, \quad e \in D_c. \quad (4)$$

The discrete counterpart of the constitutive laws is *approximate* and is written as

$$\mathbf{F} = \nu\Phi \quad (5)$$

$$\mathbf{I} = \sigma\mathbf{U} \quad (6)$$

Manuscript received December 18, 2009; revised February 23, 2010; accepted February 26, 2010. Current version published July 21, 2010. Corresponding author: R. Specogna (e-mail: ruben.specogna@uniud.it).

Color versions of one or more of the figures in this paper are available online at <http://ieeexplore.ieee.org>.

Digital Object Identifier 10.1109/TMAG.2010.2044766

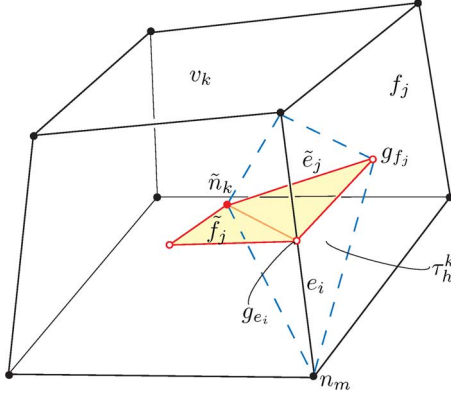


Fig. 1. Hexahedron v_k is shown, together with a primal node n_m , a primal edge e_i , and a primal face f_j , and a dual node \tilde{n}_k , a dual edge \tilde{e}_i , and a dual face \tilde{f}_j . The barycenters g_{e_i} of edge e_i and g_{f_j} of face f_j are also shown. Also the tetrahedron τ_h^k is evidenced.

where ν and σ are square symmetric positive-definite matrices ensuring consistency of equations, in the sense of Lax–Richtmyer equivalence theorem [7], and are constructed for an hexahedral primal grid in a novel way as outlined in the next section.

A symmetric algebraic system of equations, having $\mathbf{A}(t)$ as unknown, can be obtained by combining (2), (4), (5), and (6) into (1)

$$\begin{aligned} (\mathbf{C}^T \nu \mathbf{C} \mathbf{A}(t))_e &= 0, & e \in D_a \\ (\mathbf{C}^T \nu \mathbf{C} \mathbf{A}(t))_e &= \mathbf{I}_s(t)_e, & e \in D_s \\ (\mathbf{C}^T \nu \mathbf{C} \mathbf{A}(t))_e + \left(\sigma \frac{d}{dt} \mathbf{A}_c(t) \right)_e &= 0, & e \in D_c \end{aligned} \quad (7)$$

where \mathbf{A}_c contains the entries of the array \mathbf{A} relative to the edges of D_c . The source current vector $\mathbf{I}_s(t)$ can be expressed, for example, as $\mathbf{I}_s(t) = \mathbf{I}_s \cdot s(t)$,¹ where \mathbf{I}_s can be computed as described in [13] for a unit current and $s(t)$ is a function of time that describes the time evolution of the source current.

A. Integral Sources

When modeling stranded coils, it is useful to introduce integral sources, which do not require the coils to be meshed. With this aim, we express the array \mathbf{A} as $\mathbf{A} = \mathbf{A}_0 + \mathbf{A}_r$, where \mathbf{A}_0 contains the contribution produced by the source currents in D_s and \mathbf{A}_r due to the eddy currents in D_c .

Equation (7) can then be rewritten as

$$\begin{aligned} (\mathbf{C}^T \nu \mathbf{C} \mathbf{A}_r(t))_e &= 0, & e \in D_a \cup D_s \\ (\mathbf{C}^T \nu \mathbf{C} \mathbf{A}_r(t))_e + \left(\sigma \frac{d}{dt} \mathbf{A}_{rc}(t) \right)_e &= -(\mathbf{w}(t))_e, & e \in D_c \end{aligned} \quad (8)$$

where $(\mathbf{w}(t))_e = (\sigma \mathbf{A}_{0c}(ds(t)/dt))_e$. Each entry $(\mathbf{A}_{0c})_e$ of the array \mathbf{A}_{0c} can be precomputed as $(\mathbf{A}_{0c})_e = \int_e \mathbf{A}_0 \cdot d\mathbf{l}$, where e is a primal edge in D_c and \mathbf{A}_0 is the magnetic vector potential due to a unit source current in D_s .

III. DISCRETE CONSTITUTIVE RELATIONS

Each hexahedron v_k of the primal grid is partitioned in 24 tetrahedra τ_h^k , with $h = 1, \dots, 24$ (Fig. 1). Each tetrahedron

¹In general, this technique can be easily extended to more than one coil.

τ_h^k has as vertices the dual node \tilde{n}_k corresponding to v_k , the barycenter g_{f_j} of a primal face f_j on the boundary of v_k , and the two primal nodes bounding a primal edge e_i on the boundary of f_j . The label of the i th primal edge is a function of the label of the h th tetrahedron τ_h^k as $i = l^k(h)$. Similarly the label of the j th primal face of v_k is a function of the label of the h th tetrahedron τ_h^k as $j = f^k(h)$.

In the generic tetrahedron τ_h^k , we introduce a pair of triangles s_h^k and S_h^k . The triangle s_h^k has as vertices the dual node \tilde{n}_k , the barycenter of face f_j , with $j = f^k(h)$, and the barycenter of edge e_i , with $i = f^k(h)$. It is oriented as the dual face \tilde{f}_i , with $i = l^k(h)$. The triangle S_h^k has as vertices the pair of nodes bounding edge e_i , with $i = f^k(h)$ and the barycenter of face f_j , with $j = f^k(h)$. It is oriented as the primal face f_j , with $j = f^k(h)$.

The following quantities are introduced, denoted in roman type: e_i is the edge vector² corresponding to e_i , f_j is the face vector³ corresponding to f_j , \tilde{e}_j^k is the edge vector of the portion of dual edge \tilde{e}_j contained in volume v_k , and \tilde{f}_i^k is the face vector of the portion of dual face \tilde{f}_i contained in volume v_k . We will also introduce the area vectors s_h^k , S_h^k associated with s_h^k , S_h^k , respectively.

We can now define the following *piecewise uniform* vector function $v_i^e(p)$ attached to the edge e_i , defined at each point $p \in \tau_h^k$, as:

$$v_i^e(p) = \frac{s_h^k}{3|\tau_h^k|} \delta_{il^k(h)} + \left(\frac{\tilde{f}_i^k}{|v_k|} - \frac{s_h^k}{3|\tau_h^k|} e_{l^k(h)} \cdot \frac{\tilde{f}_i^k}{|v_k|} \right) \quad (9)$$

where $|v_k|$ is the volume of v^k and δ is the Kronecker delta symbol. We can also define the following *piecewise uniform* vector function $v_j^f(p)$ attached to the face f_j , defined at each point $p \in \tau_h^k$ as

$$v_j^f(p) = \frac{\tilde{e}_j^k \xi_h^k}{3|\tau_h^k|} \delta_{jf^k(h)} + \left(\frac{\tilde{e}_j^k}{|v_k|} - \frac{s_h^k}{3|\tau_h^k|} f_{f^k(h)} \cdot \frac{\tilde{e}_j^k}{|v_k|} \right) \quad (10)$$

where $\xi_h^k = |S_h^k|/|f_{f^k(h)}|$.

As shown in [6], these vector functions, constructed in a purely geometric way, possess the properties requested for constructing discrete constitutive relations for DGA by means of the energetic approach [11], [12].

Thus, the following numbers:

$$\sigma_{ij} = \int_{D_c} v_i^e \cdot \sigma v_j^e dv \quad (11)$$

$$\nu_{ij} = \int_D v_i^f \cdot \nu v_j^f dv \quad (12)$$

are the i, j entries of symmetric positive-definite constitutive matrices σ , ν , respectively, ensuring consistency and stability of discrete equations.

²Edge vector e_i is directed as the edge e_i , its amplitude is the length of e_i , and it points as the inner orientation of the edge.

³Area vector f_j is normal to face f_j , its amplitude is the area of f_j , and it points in a way congruent with the screw rule with respect to the inner orientation of the face.

Since the edge and face vector functions are piecewise uniform in v_k (i.e., uniform in each τ_h^k subregion), the volume integrals in (11) and (12) can be efficiently computed

$$\begin{aligned}\boldsymbol{\sigma}_{ij} &= \sum_{hk} v_i^e(p_h^k) \cdot \sigma v_j^e(p_h^k) |\tau_h^k| \\ \boldsymbol{\nu}_{ij} &= \sum_{hk} v_i^f(p_h^k) \cdot \nu v_j^f(p_h^k) |\tau_h^k|\end{aligned}\quad (13)$$

where $|\tau_h^k|$ is the volume of τ_h^k and p_h^k is any point in τ_h^k .

IV. TIME INTEGRATION METHOD FOR DAE PROBLEM

Systems (7) and (8) can be recast into the general form

$$\mathbf{B}\mathbf{y}' = \mathbf{a}(\mathbf{y}, t)\mathbf{y} + \mathbf{f}(t) \quad (14)$$

where array $\mathbf{y}(t)$ denotes one of the unknown arrays $\mathbf{A}(t)$ or $\mathbf{A}_r(t)$, and \mathbf{B} and \mathbf{a} are square matrices of dimension L , L being the number of primal edges in D . Their definition can be easily evinced from (7) and (8). In our eddy-current problem, matrix $\mathbf{a}(\mathbf{y}, t)$ is time invariant and independent of \mathbf{y} , the magnetic medium being linear. Matrix \mathbf{B} is time invariant and singular. In this way, (14) is not an ordinary differential equation (ODE) but rather a system of differential algebraic equations (DAEs) of C^2 class. To solve (7) or (8), we rely on an inhouse developed singly-diagonally implicit Runge–Kutta (SDIRK) DAE solver with a variable step size. In the following sections, we will summarize the implemented algorithm based on the fundamental papers [14]–[17].

A. SDIRK DAE Solver

We focus on a Runge–Kutta (R–K) method with $s = 4$ stages. In Fig. 2, we introduce an $s \times s$ matrix \mathbf{A} , and $s \times 1$ arrays \mathbf{b} , $\mathbf{c} = \mathbf{A}\mathbf{e}_s$, where \mathbf{e}_s is an array of ones $s \times 1$. The components of \mathbf{b} and \mathbf{c} are referred to as *weights* and *abscissae*, respectively. Starting from $\{\mathbf{y}_n, t_n\}$, the i th stage of an R–K method (\mathbf{A}, \mathbf{b}) is computed as

$$\mathbf{Y}_i = \mathbf{y}_n + h \sum_{j=1}^s a_{ij} \mathbf{Y}'_j, \quad i = 1, \dots, s \quad (15)$$

where \mathbf{Y}_i is the *stage value*, \mathbf{Y}'_i is the *stage derivative*, and h is the current step. The new estimate \mathbf{y}_{n+1} at $t_{n+1} = t_n + h$ is updated by

$$\mathbf{y}_{n+1} = \mathbf{y}_n + h \sum_{i=1}^s b_i \mathbf{Y}'_i. \quad (16)$$

To apply an R–K method, the following substitutions in (14) are made for the stage i : \mathbf{y} is replaced by \mathbf{Y}_i given by (15), \mathbf{y}' by \mathbf{Y}'_i , and t by $t_n + hc_i$. Thus, we obtain the following stage equation:

$$\mathbf{F}_i \left(\mathbf{Y}'_i, \mathbf{y}_n + h \sum_{j=1}^s a_{ij} \mathbf{Y}'_j \right) = 0, \quad i = 1, \dots, s. \quad (17)$$

Since in an SDIRK matrix \mathbf{A} is lower triangular, by introducing $\mathbf{W} = \mathbf{A}^{-1}$, we can invert (15) yielding the stage derivative

\mathbf{Y}'_i in terms of the stage variables \mathbf{Y}_i and the stage (17) can be rewritten as

$$\mathbf{B} \left[\sum_{j=1}^i w_{ij} (\mathbf{Y}_j - \mathbf{y}_n) \right] - h\mathbf{a}\mathbf{Y}_i - h\mathbf{f}(t_n + hc_i) = 0. \quad (18)$$

In the general nonlinear case, this stage equation is solved by means of Newton's method with stage Jacobian $\mathbf{J}_i = w_{ii}\mathbf{B} - h\mathbf{a}$. One can freely update a Jacobian to improve performance or keep the same Jacobian for several stages if it gives acceptable convergence. However, in our linear case, a linear system can be conveniently used instead.

The solution is now updated as

$$\mathbf{y}_{n+1} = (1 - \mathbf{d}^T \mathbf{e})\mathbf{y}_n + \sum_{i=1}^s d_i \mathbf{Y}_i \quad (19)$$

where $\mathbf{d}^T = \mathbf{b}^T \mathbf{W}$ and \mathbf{e} is a vector of ones $L \times 1$.

B. Error Estimation

An *embedded pair* $(\mathbf{A}, \mathbf{b}) - (\mathbf{A}, \hat{\mathbf{b}})$ of R–K methods is typically used to estimate the error in \mathbf{y} . Such a pair uses the same matrix \mathbf{A} but different advancing vectors \mathbf{b} and $\hat{\mathbf{b}}$ and related local orders⁴ k_L and \hat{k}_L . In the implemented SDIRK, (\mathbf{A}, \mathbf{b}) is accurate with $k_L = 4$ and the auxiliary SDIRK $(\mathbf{A}, \hat{\mathbf{b}})$ has $\hat{k}_L = 3$. If \mathbf{y}_{n+1} and $\hat{\mathbf{y}}_{n+1}$ are the estimates from these two methods, $k_L < \hat{k}_L$ holds, and the difference between them is typically assumed to be the local error for the (\mathbf{A}, \mathbf{b}) method

$$\mathbf{e}_{n+1} = \mathbf{y}_{n+1} - \hat{\mathbf{y}}_{n+1}. \quad (20)$$

Letting $\hat{\mathbf{d}}^T = \hat{\mathbf{b}}^T \mathbf{W}$, the local error for an embedded SDIRK pair is computed as

$$\mathbf{e}_{n+1} = (\hat{\mathbf{d}}^T - \mathbf{d}^T)\mathbf{e}\mathbf{y}_n + \sum_{i=1}^s (d_i - \hat{d}_i)\mathbf{Y}_i. \quad (21)$$

V. NUMERICAL EXPERIMENT

A fully 3-D geometry consisting of a circular coil placed above a conducting plate with conductivity $\sigma_c = 4 \cdot 10^7$ S/m is considered as a benchmark problem. Such a simple geometry is chosen to be able to compare the results with an accurate reference solution obtained by using a 2-D axisymmetric independent code (ANSYS). The geometry is shown in Fig. 3. The considered primal grid is represented in Fig. 4, where domains D_c , D_s , and D_a are shown. The source current is enforced by a stranded circular coil in D_s with a time dependence $s(t) = 400 \cdot (1 - e^{-t/\tau})$, where $\tau = 1$ ms.

To compare the results obtained with the DGA implemented in the geometric approach to Maxwell's equations (GAME) code,⁵ the ANSYS finite-elements software is used to compute reference solutions. Since the problem is axisymmetric, a reference solution has been computed with ANSYS using a 2-D quadrilateral mesh consisting of about 50 000 elements of second order (time step of 0.01 ms).

Then, a fully 3-D simulation is computed with the GAME code using the primal grid consisting of 19 136 hexahedra

⁴A time integration method is of order p if the local error depends asymptotically on the time step h as $O(h^{p+1})$.

⁵<http://www.comphys.com>

c	1/4	1/4	0	0	0	A
	11/28	1/7	1/4	0	0	
	1/3	61/144	-49/144	1/4	0	
	1	0	0	3/4	1/4	
b^T		0	0	3/4	1/4	
\hat{b}^T		-61/144	49/600	79/100	23/100	

Fig. 2. Butcher table showing the arrays A , b , \hat{b} , and c .

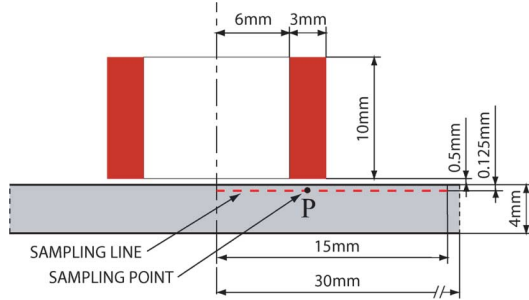


Fig. 3. Geometry of the benchmark problem, a circular coil above a conductive plate.

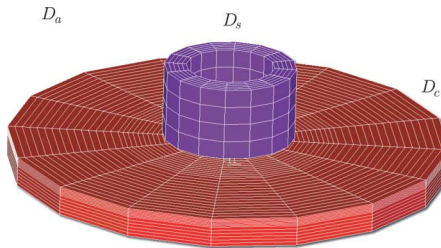


Fig. 4. Hexahedra of the considered primal grid belonging to D_c and D_s domains.

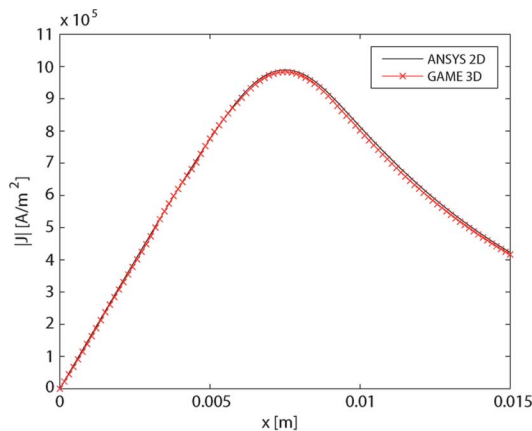


Fig. 5. Amplitude of the current densities along the sampling line shown in Fig. 3.

(59 330 DoFs) shown in Fig. 4. The GAME takes about 4 s of CPU time for the assembling of the sparse matrices and 4 s for each time step. In the implemented DAE solver, the time step is variable.

The amplitude of the current density along a number of points evenly distributed along a sampling line (shown in Fig. 3) for $t = 1$ ms is represented in Fig. 5. In Fig. 6, the time behavior of the amplitude of the current density in the point P (situated on the sampling line, at a distance of 7.5 mm from the axis) is shown. The results obtained by the GAME code are in a quite good agreement with those of ANSYS.

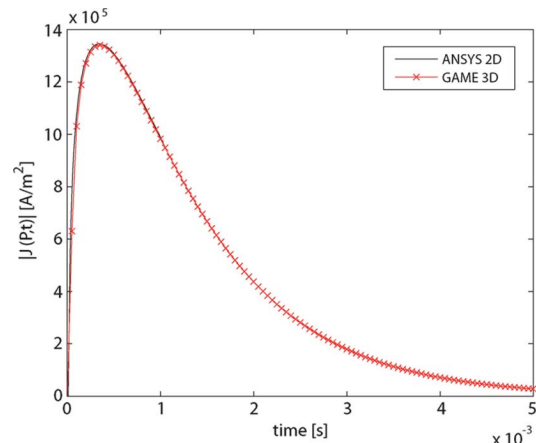


Fig. 6. Time evolution of the module of the current density in the reference point P shown in Fig. 3.

VI. CONCLUSION

A 3-D geometric time-domain eddy-current A formulation suitable with hexahedral meshes has been presented. The formulation has been successfully validated using a finite-elements commercial software.

ACKNOWLEDGMENT

The authors would like to thank M.Sc. Paolo Martin for a preliminary implementation of the DAE solver algorithm.

REFERENCES

- [1] A. Bossavit, "How weak is the weak solution in finite elements methods?," *IEEE Trans. Magn.*, vol. 34, no. 5, pp. 2429–2432, 1998.
- [2] T. Weiland, "A discretization method for the solution of Maxwell's equations for six-component fields," *Electron. Commun. (AEÜ)*, vol. 31, no. 3, p. 116, 1977.
- [3] M. Clemens and T. Weiland, "Discrete electromagnetism with the finite integration technique," *Progr. Electromagn. Res. (PIER) Monograph Ser.*, vol. 32, pp. 65–87, 2001.
- [4] E. Tonti, "Algebraic topology and computational electromagnetism," in *Proc. 4th Int. Workshop Electr. Magn. Fields*, Marseille, France, May 12–15, 1988, pp. 284–294.
- [5] E. Tonti, "Finite formulation of the electromagnetic field," *IEEE Trans. Mag.*, vol. 38, no. 2, pp. 333–336, 2002.
- [6] L. Codecasa, R. Specogna, and F. Trevisan, "Constitutive relations for discrete geometric approach over hexahedral grids," *IEEE Trans. Magn.*, accepted for publication.
- [7] A. Bossavit and L. Kettunen, "Yee-like schemes on staggered cellular grids: A synthesis between FIT and FEM approaches," *IEEE Trans. Magn.*, vol. 36, no. 4, pp. 861–867, 2000.
- [8] M. Clemens, M. Wilke, and T. Weiland, "3-D transient eddy-current simulations using $FITD$ schemes with variable time-step selection," *IEEE Trans. Magn.*, vol. 38, pp. 605–608, 2002.
- [9] M. Clemens and T. Weiland, "Magnetic field simulation using conformal FIT formulations," *IEEE Trans. Magn.*, vol. 38, pp. 389–392, 2002.
- [10] L. Codecasa, R. Specogna, and F. Trevisan, "Discrete constitutive equations over hexahedral grids for eddy-current problems," *Comput. Model. Eng. Sci.*, vol. 31, no. 3, pp. 129–144, 2008.
- [11] L. Codecasa, R. Specogna, and F. Trevisan, "Symmetric positive-definite constitutive matrices for discrete eddy-current problems," *IEEE Trans. Magn.*, vol. 43, pp. 510–515, 2007.
- [12] L. Codecasa and F. Trevisan, "Piecewise uniform bases and energetic approach for discrete constitutive matrices in electromagnetic problems," *Int. J. Numer. Meth. Eng.*, vol. 65, no. 4, pp. 548–565, 2006.
- [13] R. Specogna and F. Trevisan, "Discrete constitutive equations in $A - \chi$ geometric eddy-currents formulation," *IEEE Trans. Magn.*, vol. 41, no. 4, pp. 1259–1263, 2005.
- [14] A. Nicolet and F. Delincé, "Implicit Runge-Kutta methods for transient magnetic field computation," *IEEE Trans. Magn.*, vol. 32, no. 3, pp. 1405–1408, 1996.
- [15] F. Cameron, R. Piché, and K. Forsman, "Variable step size time integration methods for transient eddy current problems," *IEEE Trans. Magn.*, vol. 34, no. 5, pp. 3319–3322, 1998.
- [16] F. Cameron, "Low-order Runge-Kutta methods for differential-algebraic equations," Ph.D. dissertation, Tampere Univ. Technol., Tampere, Finland, 1999.
- [17] F. Cameron, M. Palmroth, and R. Piché, "Quasi stage order conditions for SDIRK methods," *Appl. Numer. Math.*, vol. 4241, pp. 61–75, 2002.